Tellus (1981), *33*, 142–161

Regional air pollution model for calculating short-term (daily) patterns and transfrontier exchanges of airborne sulfur in Europe

By CHANDRAKANT M. BHUMRALKAR, ROBERT L. MANCUSO, DANIEL E. WOLF and WARREN B. JOHNSON, *SRI International, 333 Ravenswood Ave., Menlo Park, California* 94025, *U.S.A.*, and JÜRGEN PANKRATH, *Federal Environmental Agency, Berlin (West), Federal Republic of Germany*

(Manuscript received July 3; 1979; in final form June 5, 1980)

ABSTRACT

An air pollution model, EURMAP-2, has been developed to simulate and assess the effects of daily variation in sulfur emissions on short-term (daily) air quality in central and western Europe. The model has been used to calculate daily concentrations, daily depositions, and daily transfrontier exchanges of SO_2 and $SO_4^=$ during the episodes of August 25–26 and September 14–16, 1974. A comparison between model-calculated and measured concentrations of SO_2 and $SO_4^=$ shows a reasonably good agreement over large portions of the model grid, although calculated concentrations are lower than measured values in the eastern portion. Calculated patterns for dry SO_2 deposition show strong correlation with emissions; patterns for wet deposition correspond closely to natural inhomogeneities in precipitation. Discrepancies between model results and measurements are attributed to nonrepresentativeness of emissions data in the eastern portion of the model domain and the inability of the model to realistically incorporate the effects of complex terrain, vertical diffusion, transformation, and deposition rates.

A comparison between the results of EURMAP-2 and the NILU (trajectory) model developed by the Norwegian Institute for Air Research shows some significant differences, perhaps a result of the different treatments of some physical elements in the two models.

1. Introduction

During the last two decades there has been a simultaneous growth in awareness of the quality of the environment, in the ability to measure its chemical constituents with greater accuracy and precision, and in the widespread use of mathematical models for estimating the transport and diffusion of air pollutants. In recent years, special attention has been given to problems resulting from long-range transport of air pollutants over large regional- or continental-scale areas. In many studies, theoretical models have been developed to simulate the transport, diffusion, transformation, and removal of SO_x released into the atmosphere from the multitude of sources located within a given region (for example, the studies by Eliassen and Saltbones (1974); Bolin and Persson (1975); Eliassen et al. (1976); Prahm et al. (1976); Prahm and Christensen (1977); Maul (1977); Ottar (1978) and others for Europe, and those by Rao et al. (1976); Sheih (1977) and others for the United States of America).

The EURMAP-2 model was developed as part of a study by SRI International (sponsored by the Federal Environmental Agency, Ministry of Interior, Federal Republic of Germany) to develop, evaluate, and apply a practical, quantitative technique (model) for assessing the effects of air-pollution emissions in each country in central and western Europe on the long-term (annual, seasonal, and monthly) basis as well as short-term (daily) air quality in each of the other countries.

The SRI study initially resulted in the development of a long-term model *E*uropean *R*egional *M*odel of *A*ir *P*ollution, designated as EURMAP-1 (Johnson et al., 1978). The performance and sensitivity of EURMAP-1 were evaluated by

0040-2826/81/020142-20$02.50/0

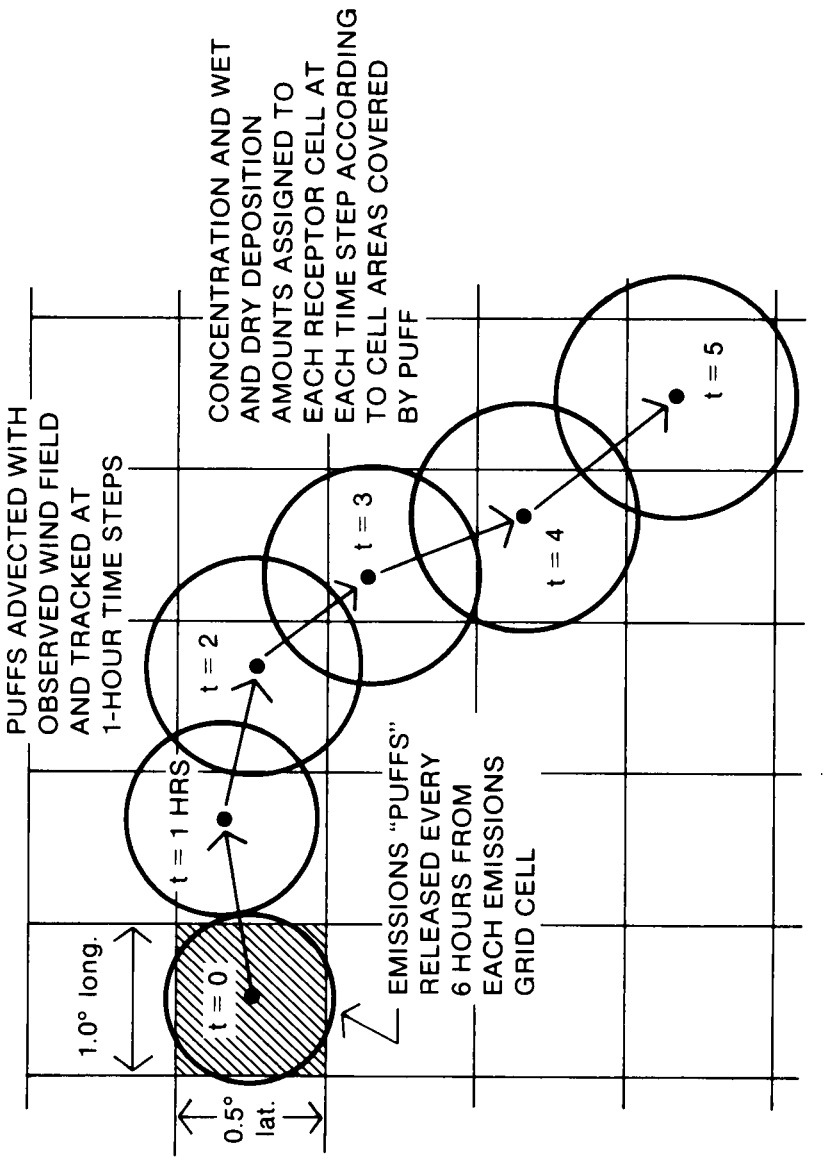

Adapted from Johnson et al (1978).

Fig. 1. Emissions puff advection in EURMAP-2.

determining the values of various parameters that gave optimum correspondence between calculated and measured values of the pollutants considered by the model (Mancuso et al., 1978). The evaluation showed that model results compare favorably with measurements if the model is modified to include higher mixing height, seasonal variations in emissions or mixing height, and a higher value for SO_2 decay rate than that used by Johnson et al. (1978).

The basic design of the short-term model EURMAP-2, which is presented in this paper, is the same as that of the long-term model EURMAP-1. The principle of operation of the EURMAP-2 model is shown in Fig. 1, adapted from Johnson et al. (1978). The EURMAP-2 model has been applied to calculate 24-h average values for two episodes in 1974 which are the same as those used by Eliassen et al. (1976) and Prahm and Christensen (1977).

2. Design of the EURMAP-2 model

The EURMAP-1 and EURMAP-2 models share several distinctive features that pertain to the calculation of long- and short-term pollution patterns. These models are designed for minimum computing requirements (and thus for economical use), yet also achieve acceptable realism in simulating the important processes in the transfrontier pollution problem. The models treat a large geographical area (2100 km N–S by 2250 km E–W); the receptor grid size is 50 km × 50 km and emitter grid size is 50 km × 70 km.

However, the long-term model was based on certain implicit assumptions that are inappropriate for the calculation of values for short-term (daily) episodes. For example, while an assumption of constant mixing height is adequate for long-term simulation, considering diurnal variations in the mixing height is very important for daily episode studies. Table 1 lists the fundamental differences between EURMAP-1 and EURMAP-2 in the treatment of pollution puffs and averaging times. As can be seen, more frequent puff emissions and a smaller time step are used in the short-term model. It may be more appropriate to choose a higher frequency for puff releases to account for rapidly changing weather conditions during a 24-h period. However, considering the magnitude of the computational requirements and the relatively low frequency at which most synoptic upper-air wind observations are available, 6-h frequency is considered to be adequate to account for contributions from relevant emission areas. Recent model sensitivity tests of EURMAP-2 have shown that the use of a more-frequent emission rate introduces relatively negligible changes in the overall results.

Table 1. *Basic differences between EURMAP-1 and EURMAP-2*

Model	Emission puff frequency (h)	Puff-tracking frequency (h)	Minimum averaging time for concentrations and deposition
EURMAP-1	12	3	1 month
EURMAP-2	6	1	1 day

Table 2 lists the differences in the treatment of some important physical elements in EURMAP-1 (long-term) and EURMAP-2 (short-term). Table 2 also lists the treatment of elements in the trajectory model NILU developed by the Norwegian Institute for Air Research (Eliassen et al., 1976).

3. Formulation of the EURMAP-2 model

3.1. *Pollutant emissions data*

The sulfur emissions data used in EURMAP-2 are from the most recent OECD-Long Range Transport of Air Pollutants (LRTAP) study (OECD, 1977), which consists of emissions data from the countries listed in Table 3. The emissions data are provided at 1° longitude by 1/2° latitude grid cells and are divided into two components—continuous and variable. The continuous emissions (E_c), which are principally industrial, are assumed to be the same throughout the year, and the variable emissions (E_v), which are principally household emissions, are assumed to have a temperature dependence. Thus, the total annual SO_2 emissions are broken down into daily emissions E given by

$$E_{\text{daily}} = \frac{E_c}{365} + \gamma \frac{DD}{TDD} E_v,$$

Table 2. *Differences in the treatment of physical elements between EURMAP-1, EURMAP-2, and NILU*

Element	Model		
	EURMAP-1	EURMAP-2	NILU
Emission data	For 13 countries	For nineteen countries; includes emissions from all countries within grid	For polar stereographic grid covering Europe (emission from south-east section excluded)
	SO_2 amount constant and based on annual total	SO_2 amount consists of constant and variable components Variable component is based on degree days	SO_2 amount constant and based on annual total
Mixing height (h)	Constant at 1 km	Varies diurnally	Constant at 1 km
Transport wind (V_T)	$V_T = 0.75 V_{850}$ $\theta = \theta_{850} - 15°$	Based on surface and 850-mb winds and a power law of the form $\frac{V_2}{V_1} = \left(\frac{Z_2}{Z_1}\right)^p$	$V_T = V_{850}$ $\theta = \theta_{850}$
Horizontal diffusion	Fickian diffusion	Based on horizontal deformation of wind field	None stated
Vertical diffusion	Immediate uniform mixing in vertical Limited up to mixing height	Not instantaneous Puff is allowed to penetrate beyond mixing height	Immediate uniform mixing in vertical
Decay rates (percent per hour)	*Dry deposition* 2.9 for SO_2 0.7 for $SO_4^=$ *Wet deposition** $21.6 \cdot R$ for SO_2 $7.0 \cdot R$ for $SO_4^=$ *Transformation* 1.0 for $SO_2 \rightarrow SO_4^=$	*Dry deposition*† $2.9/Z_p$ for SO_2 $0.7/Z_p$ for $SO_4^=$ *Wet deposition*‡ $21.6 \cdot R$ for SO_2 $7.0 \cdot R$ for $SO_4^=$ *Transformation*‡ 1.0 for $SO_2 \rightarrow SO_4^=$	*Decay rate* 5.4 for SO_2 1.44 for $SO_4^=$ *Transformation* 0.72 for $SO_2 \rightarrow SO_4^=$

* R is rainfall rate in mm/h.
† Z_p is the height of the top of the puff in km.
‡ Same as EURMAP-1.

where

E_c = the annual amount of continuous SO_2 emissions
E_v = the annual amount of variable SO_2 emissions
DD = degree-days
= $18 - \bar{T}$ °C for $\bar{T} < 18$ °C (where $\bar{T}$ = daily mean temperature in °C)
TDD = total degree-days over a specified period (August 1974)
γ = fraction of the annual variable emission emitted during the specified period. In this study, for the specified periods of August and September, γ has been estimated to be 0.14 on the basis of seasonal emission curves given by OECD (1977) pp. 2–17.

3.2. *Mixing height*

In EURMAP-2 the mixing height, which is an important parameter for determining the vertical growth of a pollutant puff during the course of a given day, is allowed to vary diurnally. For this purpose, 0000 and 1200 GMT radiosonde data at 48 stations located within the model domain have been used. The procedure for calculating mixing

Table 3. *Countries whose emissions data have been used in EURMAP-2*

Number	Country
1	Austria
2	Belgium
3	Czechoslovakia
4	Denmark
5	Federal Republic of Germany (FRG)
6	France
7	German Democratic Republic (GDR)
8	Hungary
9	Italy (north of 42° N)
10	Norway (south of 60° N)
11	Poland
12	Romania
13	Spain (north of 42° N)
14	Sweden (south of 60° N)
15	Switzerland
16	The Netherlands (Holland)
17	Union of Soviet Socialist Republics (Russia, west of 25° E)
18	United Kingdom (U.K.) and Ireland
19	Yugoslavia

height in EURMAP-2 consists of the following steps.

(a) Daily minimum mixing height is obtained at each station. This is defined as the height of lowest temperature-inversion indicated by 0000 GMT sounding.

(b) Daily maximum mixing height is obtained at each station following the procedure described by Holzworth (1972). This is defined as the height at which the dry adiabatic extension from the maximum surface temperature observed at 1200 GMT intersects the 0000 GMT radiosonde sounding.

(c) The diurnal variation at each station is obtained by linearly interpolating between the minimum and maximum values of the mixing heights.

(d) Spatial distribution of mixing heights is obtained by performing an objective analysis for the values at the stations located within the model domain.

An example of the diurnal variation of mixing height in EURMAP-2 is shown in Fig. 2.

Although the use of 0000 and 1200 GMT sounding to obtain mixing height is perhaps not as appropriate in Europe as in the United States, the procedure (followed in EURMAP-2) has been used widely in the United States and has yielded results that are in good agreement with observations (Holzworth, 1972).

3.3. *Pollutant transport wind*

In EURMAP-2 wind is divided into surface-layer wind, from surface (10 m) to h_s, and an upper-layer wind, from h_s to 850 (~1500 m), where h_s, the height of the surface layer, is set at 300 m.

The winds in the two layers are calculated by applying a power law of the form

$$\frac{V_2}{V_1} = \left(\frac{Z_2}{Z_1}\right)^p \tag{2}$$

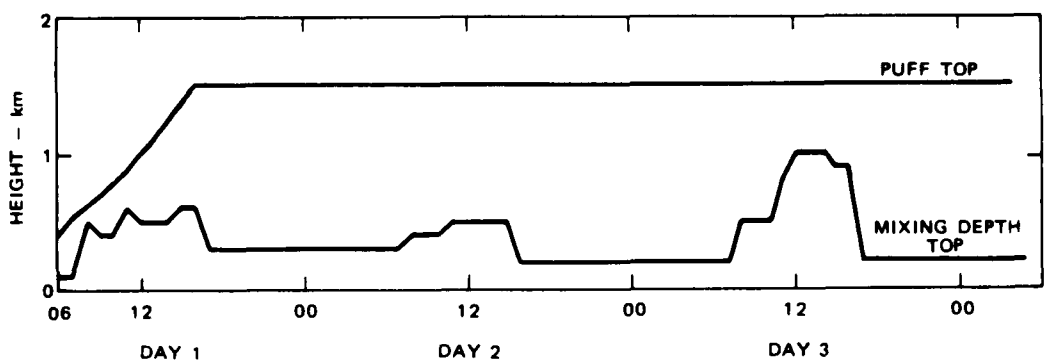

Fig. 2. Diurnal variations of mixing height to EURMAP-2.

where V_2 and V_1 are wind speeds at height Z_2 and Z_1, respectively. p is a dimensionless empirical parameter that is determined as a function of stability following Touma (1977). Equation (2) is used to calculate integrated wind speeds in each layer by using the observed surface wind for the lower surface layer and observed 850-mb wind for the upper layer. The wind directions in the upper and surface layers are considered to be the same as 850-mb and surface-wind directions, respectively, and the wind speeds and directions obtained for the surface and upper layers are converted to u and v wind components.

The transport wind components (u_t and v_t) that move the pollutant puffs are derived from the u and v wind component of the surface and upper layers. The component u_t of the transport wind is calculated by the formula

$$u_t = \frac{h_s \cdot u_s + (Z_p - h_s)u_u}{Z_p}, \tag{3}$$

where

Z_p is the puff height ($Z_p \geq h_s$)
h_s is the height of the surface layer
u_s is the u component of the surface layer wind
u_u is the u component of the upper layer wind.

The component v_t of the transport wind is calculated by a formula similar to eq. (3), which shows that the transport wind used in EURMAP-2 is a weighted mean between surface and upper layer winds and depends on the puff height Z_p. This technique does not account for the error introduced by convergence and divergence in the wind field. This error has not been quantified in this study.

3.4. *Horizontal diffusion*

In EURMAP-2, the horizontal diffusion of the material in the puff is calculated by using the formula

$$A = A_0 + K_H t, \tag{4}$$

where A_0 is the initial area of the puff, and K_H is the horizontal diffusion coefficient. K_H is estimated by using a nonlinear formulation following Keyser and Anthes (1977):

$$K_H \propto (DS)^2 D, \tag{5}$$

where DS is grid length and D is deformation in horizontal wind, given by

$$D = \left[\left(\frac{\partial u}{\partial x} - \frac{\partial v}{\partial y}\right)^2 + \left(\frac{\partial v}{\partial x} + \frac{\partial u}{\partial y}\right)^2\right]^{1/2}.$$

3.5. *Vertical diffusion of pollutant's puffs*

In EURMAP-2, the puff initially extends from the surface to a height of 400 m, following Fisher (1975), who has indicated that about half of the sulfur emissions are from sources whose effective height in summer could be as high as 400 m. To determine a puff's vertical growth, a stability class is first determined from observed meteorological data by using the Pasquill scheme developed for categorizing stability for rural areas (Turner, 1970). Then, following a procedure similar to that described by Ludwig et al. (1978), a puff is allowed to grow vertically according to a stability class pertinent to the time and location of the puff. As the puff grows and penetrates the mixing height its growth above the height is continued on the basis of the stability that is one class higher (i.e., more stable) than that existing below the mixing height. The rationale for this procedure is that, in the real atmosphere, although a pollutant puff can penetrate beyond the mixing height (Goodman and Miller, 1977), the atmosphere immediately above is more stable than that below the mixing height, and the puff's growth will therefore be slower above than below it. The maximum height up to which a puff is allowed to grow is 1.5 km, which, on the basis of curves drawn by Turner (1970), corresponds to a horizontal travel distance of 1000 km. We believe that at this stage the puff is either off the model grid or is so depleted that its contribution is relatively small, and it is not meaningful to track it any further.

3.6. *Decay coefficients for SO_2 and $SO_4^=$*

The wet deposition (k_w) and transformation (k_T) coefficients in both EURMAP-1 and EURMAP-2 are the same. However, in EURMAP-2, the dry deposition coefficient is calculated from the formula

$$k_d = w/Z_p, \tag{6}$$

where

k_d = dry deposition coefficient (percent per hour)
w = constant deposition velocity (km per hour)
Z_p = puff height (km).

Equation (6) implies that the decay of pollutant due to dry deposition is proportional to concen-

tration. Thus, more pollutant material is lost during the initial life of the puff, when Z_p is small. The values of k_w, k_T, and other parameters used in calculating decay rate are given in Table 2. These values are based upon the best available state-of-the-art information and have been used in other model applications (Johnson et al., 1978). The values, however, are not certain and should be considered only tentative.

4. Data base used in EURMAP-2 calculations and evaluation

4.1. *Episodes selected for EURMAP-2 calculations*

In general, an episode connotes only a relative measure and is not related to the total pollution in a given area or at a given site. OECD (1977) has defined episodes on the basis of daily sulfate wet depositions at a given site and identified some days in August and September 1974 when there were high depositions of sulfate. We have performed EURMAP-2 calculations for the two episodes—August 25 and 26 and September 14, 15, and 16, 1974—that were identified by the sponsor.

4.2. *Emissions data*

Fig. 3 shows a graphical display of the annual sulfur emissions used in this study. These emissions have been derived from the data provided by OECD (1977). The figure shows that the highest emissions lie in a broad band extending from the central United Kingdom east–southeastward to southwestern Poland, encompassing most of the heavily industrialized regions in the study area.

There are certain limitations in the use of the emissions data for simulating short-term (daily) sulfur concentrations and depositions. Not all the countries in LRTAP supplied emissions data strictly according to specifications. Thus, the data from different countries are not always comparable. In addition, the emissions data do not identify details necessary for studying short-term conditions; for example, the heights of emissions over the study area are not known. Thus the emissions data are useful only for calculating large-scale atmospheric dispersion and are perhaps not quite suitable for evaluations on a scale of less than 100 km between significant points (Rystad et al., 1974).

4.3. *Meteorological data*

In this study we have used 1974 meteorological data from upper air and surface stations over Europe that were obtained from the National Climatic Center, Asheville, North Carolina, U.S.A. The number of stations from which data were actually available ranged up to 48 for upper air and up to 600 for surface. The grid point values of meteorological input parameters such as mixing height, transport wind, horizontal diffusion coefficient, temperature, rainfall rate, and atmospheric stability have been derived from these available observed data following objective analysis techniques developed by Endlich and Mancuso (1968). The temporal values of these parameters were obtained by linear interpolation between the values at 0000 GMT and 1200 GMT. The rainfall rates over land areas were computed from the surface reports that contained rainfall data. Since no rainfall measurements were available over the North Sea, these were approximated by distance-weighted interpolation and extrapolation of the rainfall data at the land stations located at the coasts of the countries contiguous to the North Sea.

Synoptic weather maps for August and September 1974 were also used to provide a description of large-scale meteorological conditions to aid in interpreting the results from the model runs.

4.4. *Air quality data*

The air quality data used within this study have been taken from the data base of the OECD program (NIAR, 1975). These data consist of 24-h average values of SO_2 and $SO_4^=$ air concentrations for the two episodes, August 24–26 and September 14–16, in 1974. The actual data used in the EURMAP-2 model evaluations, are those

(a) that fall within the domains covered by both EURMAP-2 and NILU (Eliassen et al., 1976) models. However, for consistent comparison between NILU and EURMAP-2 models, some data from NILU model domain that fall outside the EURMAP-2 model domain have been excluded.
(b) that were considered to be consistent with the data at surrounding locations. This subjective criteria resulted in the exclusion of only 2 stations in two days of the August episode and 4 stations in the three-day September episode.

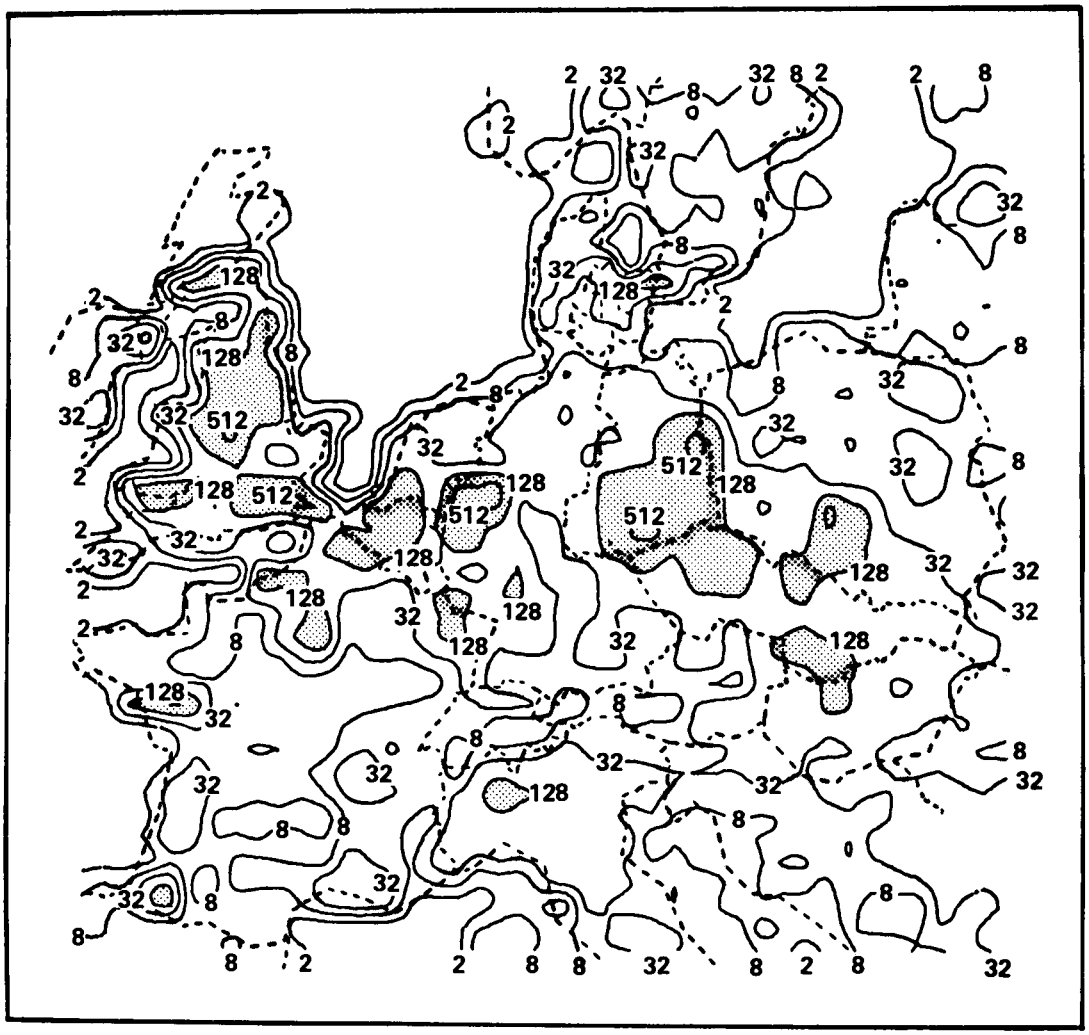

Fig. 3. Annual emissions of sulfur over Europe for 1973 (10^{-1} ton S/km^2).

Also, following the recommendation of OECD (1977), we excluded measured SO_2 concentration values from the locations in Denmark.

5. EURMAP-2 model results

Using the emission data shown in Fig. 3 and the corresponding meteorological data, EURMAP-2 calculations were performed to obtain SO_2 and $SO_4^=$ concentrations and depositions for the two-day (25–26) episode in August 1974 and the three-day (14–16) episode in September 1974.

EURMAP-2 was initialized by calculating the concentrations and depositions for five days *preceding* the first day of the episode, to obtain a realistic representation of actual puffs existing at the start of the episode and to minimize the unrepresentative results that may occur if the model is started from the first day of the episode. The five-day period, though arbitrary, was determined by performing several tests.

5.1 *Results of episode of August* 25–26, 1974

5.1.1. *Meteorological conditions.* The synoptic weather maps for August 25–26, 1974, showed winds predominantly south–southwesterly over

the United Kingdom, North Sea, and western Scandinavia. This circulation was caused by a low-pressure area over southeastern Iceland. Also, a high-pressure cell over the eastern part of the model domain caused a weaker east–southeasterly flow that merged with the westerly flow over Denmark and southern Sweden. The observed rainfall patterns indicated that rainfall was confined to the United Kingdom and southern Norway on August 25. However, on August 26 rain fell over more extensive areas in the north-western and southeastern parts of Europe, but almost no rainfall was recorded over France, the GDR and Poland.

5.1.2. *Comparison between calculated results and measurements.* EURMAP-2 model results have been compared with the air quality measurements discussed in Section 4.4. Fig. 4 shows calculated and measured concentrations for SO_2 and $SO_4^=$; the measured values are shown in circles. Note the logarithmic contour intervals (2, 4, 8, 16, 32) used in depicting calculated results.

In general, SO_2 concentrations calculated by EURMAP-2 appear to be lower than the measured values in the United Kingdom, Denmark, and eastern Sweden (Fig. 4(a)). However, in some regions, calculated results are in good agreement with measured values. For example, in Holland and

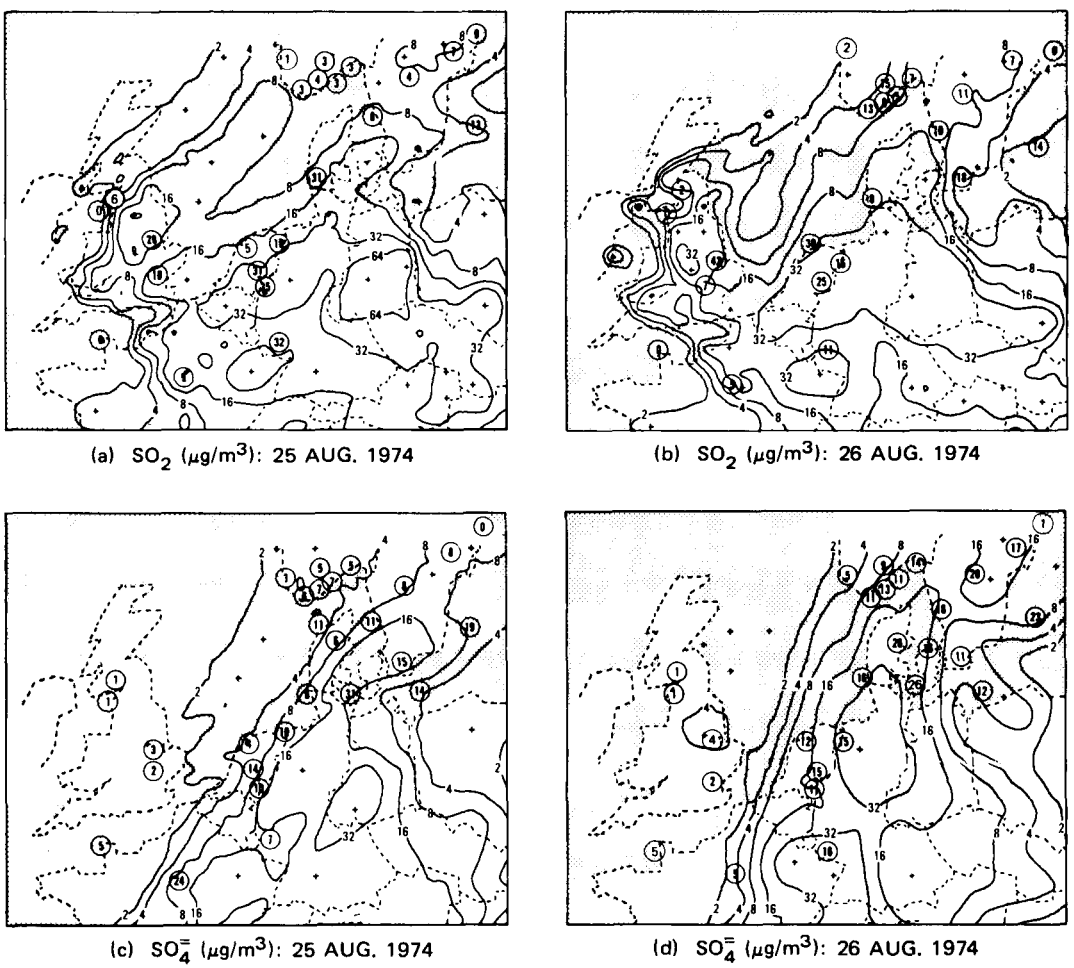

Fig. 4. Calculated and measured concentrations of SO_2 and $SO_4^=$ for August 25 and 26, 1974.

Table 4. *Comparison between EURMAP-2 model-calculated and measured concentrations for SO_2 and $SO_4^=$ for August 1974 episode*

	25 August		26 August	
Pollutant	r	r.m.s.e. ($\mu g/m^3$)	r	r.m.s.e. ($\mu g/m^3$)
SO_2	0.70	13.7	0.5	14.4
$SO_4^=$	0.61	5.9	0.68	7.4

northern FRG, measured values of 31 and 35 $\mu g/m^3$ are quite close to the calculated contour for 32 $\mu g/m^3$. Similarly, the calculated and measured values show good agreement in southern Norway.

The calculated $SO_4^=$ concentrations show a relatively better agreement with measured $SO_4^=$ concentrations (Fig. 4(c) and (d)). For example, on August 26, 1974, the measured and calculated concentrations in the United Kingdom, the Netherlands, and southern Norway agree quite well. The calculated values show a large deviation from measured values in the eastern part of the model domain and in southern Denmark and eastern Holland. This discrepancy between calculated and measured values can be attributed to the non-availability of emissions data from large areas of the USSR. This is particularly important because the transport wind during this episode was from the east.

Table 4 shows correlation coefficient (r) and root mean square errors (r.m.s.e.) between the calculated and measured values for the August episode. Overall, the calculated values for SO_2 correlated reasonably well with measurements on August 25, although on August 26 the r value is 0.5. The r.m.s.e. values shown in the table are about 1/10 of the peak calculated values.

5.1.3. *Deposition results.* Fig. 5 shows calculated SO_2 dry (left) and wet (right) depositions from emissions in central and western Europe for August 25 and 26, 1974. A comparison of the patterns of calculated SO_2 concentrations and dry deposition shows that they are quite similar, with high concentrations and high dry depositions occurring in regions of high emissions. This result is consistent with the fact that in a given high-emission cell, the initial concentration of pollutants in a puff released from the cell will be large. At the same time, because the initial puff height is small, the dry deposition rate as computed from eq. (6) will be large, and thus a higher amount of pollutant will be deposited in this location of high emission. Then, as the puff advects downwind and grows in height, both its concentration and dry deposition rate decrease. As a consequence, the dry deposition is less in regions away from high-emission areas.

The wet deposition patterns of SO_2 (Fig. 5) reflect the normal inhomogeneities in the spatial distribution of precipitation. The wet depositions for August 25 and 26 correspond to the rainfall pattern for these two days. As in the case of SO_2, the dry deposition patterns for $SO_4^=$ are similar to $SO_4^=$ concentration patterns.

5.1.4. *Transfrontier exchanges.* Table 5 shows the total sulfur depositions (in tons) that came from emissions from each of the nineteen countries during the two-day August episode. The values along the diagonal of the matrix represent the amounts emitted by each country and the amount deposited within the country itself. For example, 2238 tons of total sulfur deposition within FRG came from emissions from FRG itself. The table also shows the amount received by each receptor country from other emmiter countries. For example, Switzerland receives a total of 345 tons of sulfur from itself and other 18 countries. Out of this it receives 32 tons from itself, 117 tons from Czechoslovakia and only 11 tons from Austria. The table also shows the amount received by receptor countries from a given emitter country. For example, Switzerland gives 14 tons to France and only 1 ton to Austria. (The authors wish to emphasize that since the EURMAP-2 model has not yet been verified and validated, the results shown in Table 5 are preliminary only.)

5.2. *Results of episode of September 14 to 16, 1974*

Results of EURMAP-2 calculations were also performed to obtain pollutant concentrations and depositions for the three-day episode of September 14–16, 1974. The emission data used in these simulations were the same as those used in simulating the August episode (Fig. 3).

5.2.1. *Meteorological conditions.* An examination of synoptic daily weather maps for the September, 14–16, 1974, episode given by Eliassen et al. (1976) showed that on September 13 a front extended from north of the United Kingdom to north of Italy, located between the United King-

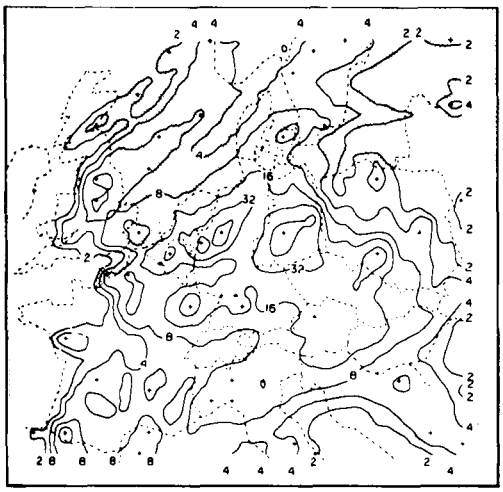

(a) SO_2 DRY DEPOSITION (mg/m^2): 25 AUG 1974

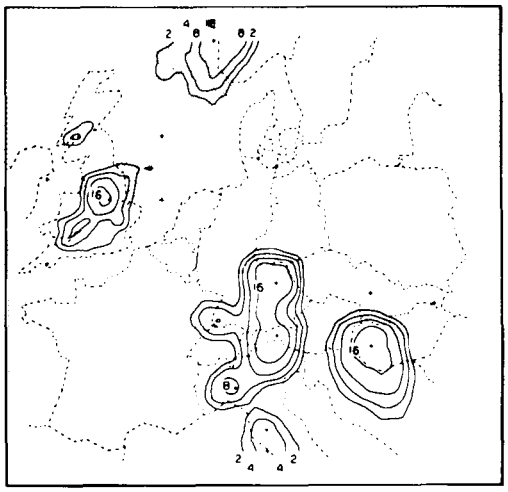

(b) SO_2 WET DEPOSITION (mg/m^2): 25 AUG. 1974

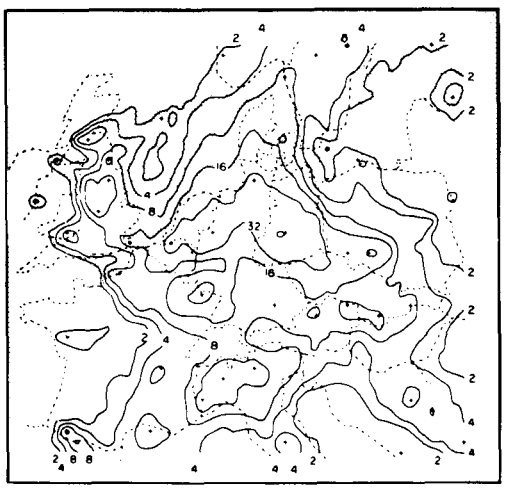

(c) SO_2 DRY DEPOSITION (mg/m^2): 26 AUG. 1974

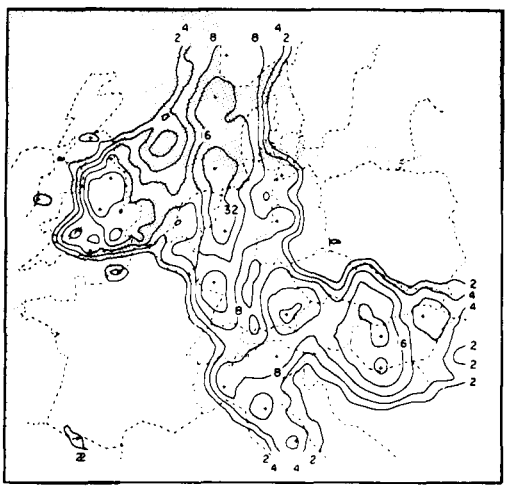

(d) SO_2 WET DEPOSITION (mg/m^2): 26 AUG. 1974

Fig. 5. Calculated SO_2 dry and wet depositions from emissions in central and western Europe for August 25 and 26, 1974.

dom and Scandinavian countries. The front moved over Norway and Denmark on September 14 and remained stationary in that region. On September 16, an occluded front appeared over the United Kingdom with another front ahead of it over the North Sea. During the entire episode, a high-pressure anticyclonic cell was located to the east of the front. Rainfall occurred over the United Kingdom on all three days; on September 15 and 16, the rainy area extended to southwestern Norway and a portion of France.

5.2.2. *Comparison between calculated results and measurements.* Figs. 6 and 7 show calculated and measured concentrations for SO_2 and $SO_4^=$ respectively (measured values of SO_2 and $SO_4^=$ are in circles).

An examination of measured SO_2 concentration (Fig. 6) shows that high SO_2 concentrations were

Table 5. *Contributions to total sulfur depositions on August 25 and 26, 1974, based on emissions from each of the 19 countries used in the EURMAP-2 model calculations (metric tons)*

	Total contributions to S depositions within receptor countries																		
Emitter country	1	2	3	4	5	6	7	8	9	10	11	12	13	14	15	16	17	18	19
August 25, 1974																			
1 FRG	2238	104	447	1	3	44	38	25	0	6	0	21	59	0	7	0	66	0	0
2 GDR	1000	1857	132	36	113	2	0	0	0	1	0	22	70	0	6	0	12	0	0
3 France	44	0	1455	0	0	1	30	115	0	0	0	0	12	0	1	0	121	0	0
4 Poland	140	268	14	1083	521	0	0	0	0	0	0	302	29	22	198	23	1	9	0
5 Czechoslovakia	647	133	18	35	864	0	0	0	0	0	0	531	117	104	445	73	1	0	0
6 Denmark	1	6	1	40	0	62	0	0	0	59	0	0	0	0	0	0	0	28	0
7 Holland	104	2	41	0	0	41	130	6	0	4	0	0	0	0	0	0	18	0	0
8 Belgium	220	0	114	0	0	9	135	211	0	0	0	0	0	0	0	0	35	0	0
9 U.K. + Ireland	47	0	169	0	0	206	72	7	1020	328	303	0	0	0	0	0	33	7	0
10 S. Norway	0	0	0	7	0	0	0	0	0	98	0	0	0	0	0	0	0	27	0
11 S. Sweden	0	0	0	0	0	0	0	0	0	7	15	0	0	0	0	0	0	0	0
12 Austria	28	0	4	0	1	0	0	0	0	0	0	185	11	3	167	18	0	0	0
13 Switzerland	1	0	14	0	0	0	0	0	0	0	0	1	32	0	3	0	0	0	0
14 Hungary	0	0	1	0	20	0	0	0	0	0	0	106	0	594	111	241	0	1	4
15 N. Italy	0	0	56	0	0	0	0	0	0	0	0	2	15	0	667	0	0	0	0
16 Yugoslavia	0	0	0	0	0	0	0	0	0	0	0	2	0	40	135	802	0	0	6
17 N. Spain	0	0	1	0	0	0	0	0	0	0	0	0	0	0	0	0	20	0	0
18 W. Russia	0	2	0	32	25	0	0	0	0	0	0	12	0	68	2	4	0	151	7
19 Romania	0	0	0	0	0	0	0	0	0	0	0	6	0	137	10	132	0	0	83
Total (tons S)	4470	2373	2467	1234	1547	366	405	364	1020	502	318	1189	345	967	1752	1292	307	223	100

August 26, 1974

1	FRG	2533	47	372	0	4	280	400	69	0	72	62	8	27	0	0	0	16	0	0
2	GDR	1606	1325	177	13	9	351	3	1	0	28	11	1	26	0	1	0	6	0	0
3	France	171	0	1342	0	0	5	138	207	0	0	3	0	11	0	2	0	122	0	0
4	Poland	596	524	20	1087	399	75	0	0	0	12	1	100	112	7	114	0	1	6	0
5	Czechoslovakia	871	392	66	62	1158	0	0	0	0	0	0	334	168	71	240	1	1	0	0
6	Denmark	0	1	1	13	0	65	0	0	0	68	28	0	0	0	0	0	0	19	0
7	Holland	37	1	21	0	0	38	135	7	0	37	36	0	0	0	0	0	7	0	0
8	Belgium	126	0	58	0	0	31	277	175	0	6	14	0	0	0	0	0	4	0	0
9	U.K. + Ireland	7	0	102	0	0	67	19	22	2341	207	428	0	0	0	0	0	24	11	0
10	S. Norway	0	0	0	5	0	0	0	0	0	107	7	0	0	0	0	0	0	9	0
11	S. Sweden	0	0	0	0	0	0	0	0	0	1	17	0	0	0	0	0	0	0	0
12	Austria	172	0	11	0	15	0	0	0	0	0	0	310	37	3	88	10	0	0	0
13	Switzerland	7	0	18	0	0	0	0	0	0	0	0	3	51	0	4	0	0	0	0
14	Hungary	10	0	4	0	129	0	0	0	0	0	0	273	1	797	287	85	0	2	9
15	N. Italy	0	0	108	0	0	0	0	0	0	0	0	3	47	0	1063	0	0	0	0
16	Yugoslavia	0	0	1	0	0	0	0	0	0	0	0	10	1	124	200	978	0	0	11
17	N. Spain	0	0	2	0	0	0	0	0	0	0	0	0	0	0	0	0	26	0	0
18	W. Russia	8	2	0	63	94	1	0	0	0	0	0	43	1	74	16	1	0	164	14
19	Romania	0	0	0	0	5	0	0	0	0	0	0	12	0	168	61	107	0	1	176
Total (tons S)		6143	2292	2304	1244	1814	913	971	481	2341	538	604	1098	481	1244	2076	1182	207	212	210

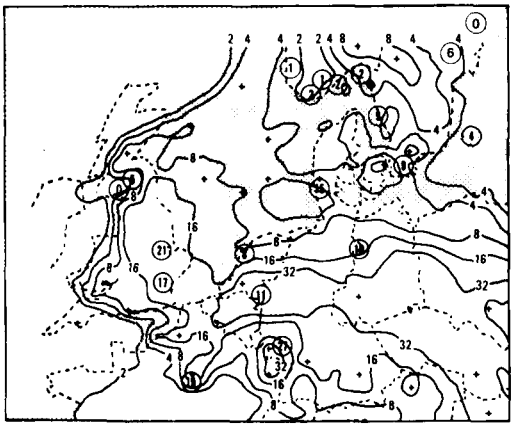

(a) SO_2 CONCENTRATION ($\mu g/m^3$), 14 SEP. 1974

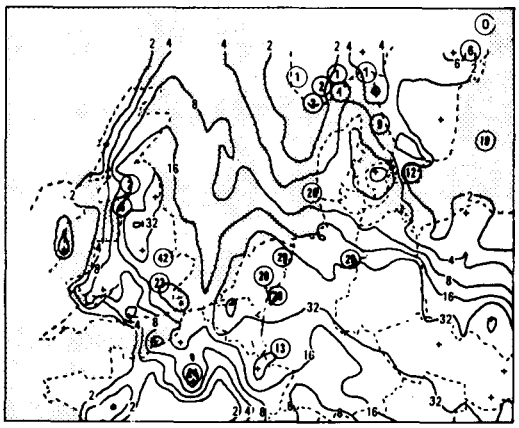

(b) SO_2 CONCENTRATION ($\mu g/m^3$), 15 SEP. 1974

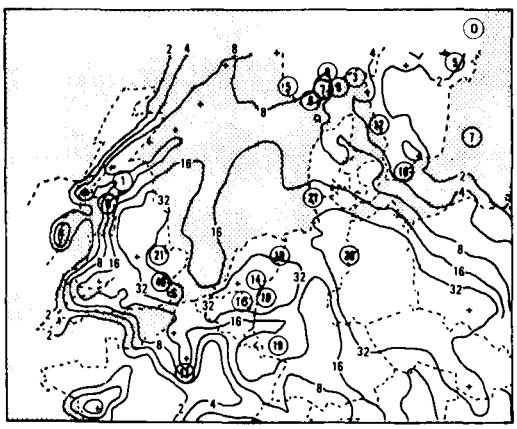

(c) SO_2 CONCENTRATION ($\mu g/m^3$), 16 SEP. 1974

Fig. 6. Calculated and measured concentrations of SO_2 for September 14 to 16, 1974.

measured in high emission areas and that the SO_2 concentrations are relatively low in low emission areas with several stations recording zero values.

A comparison between measured SO_2 and $SO_4^=$ concentrations during this episode shows that in the United Kingdom and the Netherlands/northern FRG regions, high concentrations of both SO_2 and $SO_4^=$ were measured on all three days of the episode. In the Norway and the Denmark/southern Sweden regions, however, although SO_2 concentrations were relatively small on all days of the episode, high $SO_4^=$ concentrations were measured on September 16.

The preceding discussion implies that whereas there is good correspondence between high SO_2 and high $SO_4^=$ concentrations in the U.K. and the Netherlands-FRG areas, such is not the case in southern Norway and the Denmark/southern Sweden regions. These differences can be attributed to the differences in the relative importance of the transport and transformation processes. For example, in the United Kingdom and the Netherlands/FRG areas, the stagnant meteorological conditions cause local transformation to be more effective than transportation, which results in high SO_2 and $SO_4^=$ concentrations. However, in southern Norway and the Denmark/southern Sweden regions, the atmospheric transport predominates, and thus $SO_4^=$ measured in this region is not strongly influenced by locally emitted SO_2.

A comparison of computer-run results with measured values of SO_2 concentrations shows that

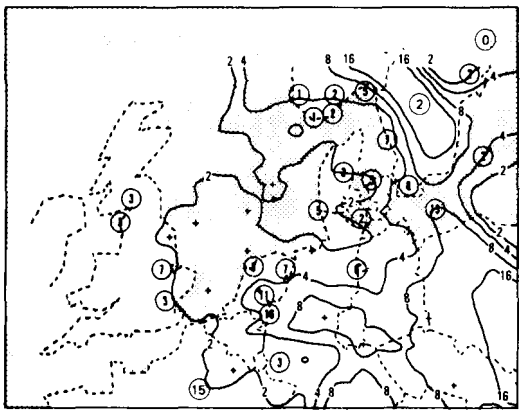

(a) $SO_4^=$ CONCENTRATION ($\mu g/m^3$), 14 SEP. 1974

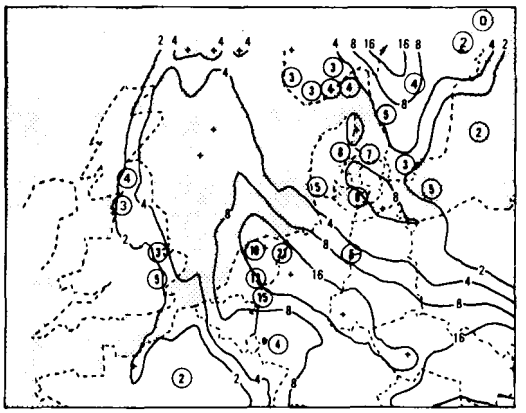

(b) $SO_4^=$ CONCENTRATION ($\mu g/m^3$), 15 SEP. 1974

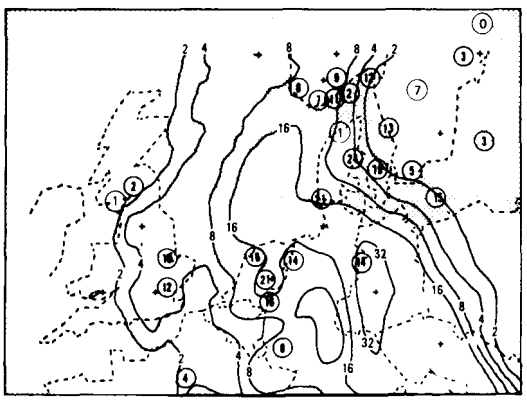

(c) $SO_4^=$ CONCENTRATION ($\mu g/m^3$), 16 SEP. 1974

Fig. 7. Calculated and measured concentrations of $SO_4^=$ for September 14 to 16, 1974.

the model results are in good agreement with measurements in the United Kingdom area. For example, September 14, a contour line representing 16 $\mu g/m^3$ of SO_2 concentration encompasses measured values of 21 and 17 $\mu g/m^3$. On September 15, measured values of 20 and 29 $\mu g/m^3$ are close to the calculated contour value for 32 $\mu g/m^3$.

A comparison between calculated and measured $SO_4^=$ concentrations (Fig. 7) shows reasonable agreement in the United Kingdom and Netherlands/northern FRG areas. In the Denmark/southern Sweden region, the model results for September 14 and 15 show reasonable agreement with measured values, though on September 14, model calculated maximum is much higher than the maximum measured concentration in this region. The model calculated values for September 16 are also much lower than those measured on this date. This discrepancy can be explained on the basis of transport winds and emissions data used in EURMAP-2. For example, an examination of the transport winds used in the model for the September episode (Fig. 8) shows the following sequence:

(a) On September 14 some pollutant puffs entering the Denmark/southern Sweden region originated in the United Kingdom (a region with significant emissions). Other puffs originate from the eastern portion of the model domain where no emissions data are available.
(b) On September 15, the winds over Denmark are generally southerly, as shown in Fig. 8(b); puffs are being transported into this region predominantly from regions with no emissions data.

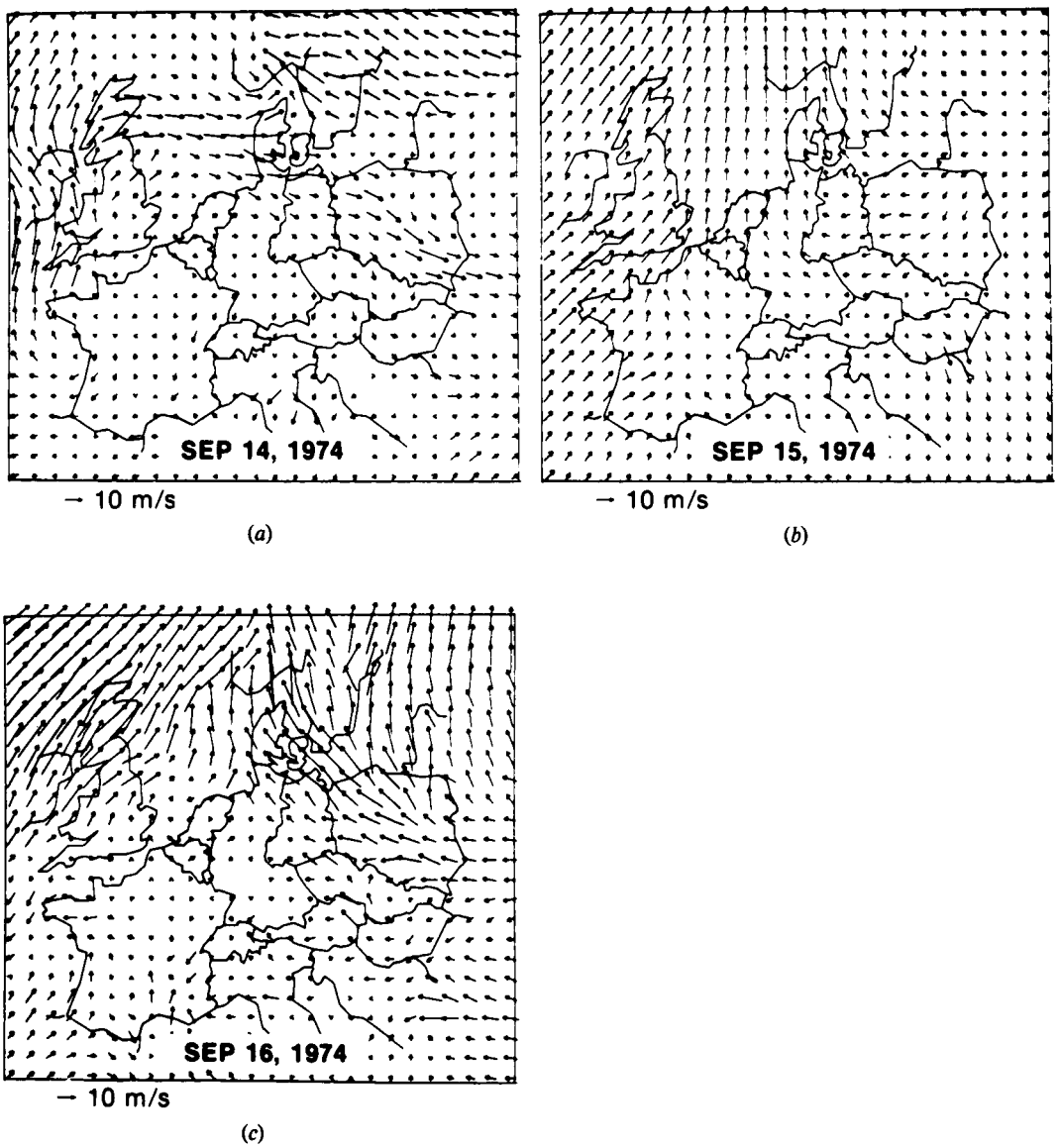

Fig. 8. Transport winds used in EURMAP-2 for calculating concentrations for September 14 to 16, 1974.

(c) On September 16, Fig. 8(c), the Denmark/southern Sweden area is characterized by strong winds. The above sequence of events implies that in the EURMAP-2 calculations, the concentration of pollution within puffs reaching the Denmark/southern Sweden region from the east tends to be underestimated because of the lack of emissions data from western U.S.S.R. Also, it appears that the strong transport winds obtained by eq. (3) cause SO_2 to move rapidly out of the Denmark/southern Sweden region, thereby reducing its "residence time" in the region. This, in turn, does not leave enough SO_2

Table 6. *Comparison between EURMAP-2 model-calculated and measured concentrations for SO_2 and $SO_4^=$ for September 1974 episode*

	September 14		September 15		September 16	
Pollutant	r	r.m.s.e. ($\mu g/m^3$)	r	r.m.s.e. ($\mu g/m^3$)	r	r.m.s.e. ($\mu g/m^3$)
SO_2	0.53	11.2	0.5	21.9	0.61	18.0
$SO_4^=$	0.41	4.6	0.86	2.8	0.41	7.7

pollutant for transformation into $SO_4^=$, and whatever $SO_4^=$ is formed is flushed out of the region by the strong transport winds.

Table 6 shows r and r.m.s.e. values between calculated and measured values for the period September 14–16, 1974. Overall, the correlation between calculated and measured values for the September episode is not as good as that for the August episode (Table 4).

5.2.3. *Deposition results.* The dry and wet deposition patterns for SO_2 and $SO_4^=$ for the September episode are similar to those for August 25 and 26, 1974 (shown in Fig. 6). For example:

(a) SO_2 dry depositions are strongly influenced by the emissions (and therefore concentration) distribution, with maxima generally corresponding to the emissions field.
(b) The wet deposition patterns correspond closely to the natural inhomogeneities in precipitation.
(c) $SO_4^=$ depositions are generally displaced downwind of SO_2 source areas, as would be expected by virtue of the finite time required for transformation of SO_2 to $SO_4^=$.

6. Comparison between EURMAP-2 and NILU (Trajectory) model results

In addition to EURMAP-2, the daily patterns of sulfur pollutants over central and western Europe for the two episodes used in this study have been calculated by the NILU (Trajectory) model developed by the Norwegian Institute for Air Research (Eliassen et al., 1976) and the pseudo-spectral dispersion model (PDS) developed at the Danish Meteorological Institute (Prahm and Christensen, 1977). In this study, we have compared the EURMAP-2 results with those of NILU as discussed below.

Table 7. *Comparison between NILU-calculated and measured concentrations for SO_2 and $SO_4^=$ for August 1974 episode*

	August 25		August 26	
Pollutant	r	r.m.s.e. ($\mu g/m^3$)	r	r.m.s.e. ($\mu g/m^3$)
SO_2	0.80	6.6	0.64	6.7
$SO_4^=$	0.51	7.0	0.64	6.7

NILU is a trajectory model that has been applied to compute daily pollution patterns over central and western Europe for the two episodes during August and September 1974 discussed in Section 5.

Table 7 shows the r and r.m.s.e. values between calculated and measured $SO_4^=$ concentrations on August 25 and 26, 1974, as derived from NILU model results. These have been obtained by using the calculated and measured values given by Eliassen et al. (1976). However, for the purpose of comparison with EURMAP-2 results, certain portions of the NILU domain that fell outside the EURMAP-2 domain have been excluded; this accounts for the differences between the r values shown in Table 7 and those listed in Tables C-4 through C-6 of Eliassen et al. (1976). (A similar procedure was also adopted for the September episode.)

A comparison of r and r.m.s.e. values for NILU with those of EURMAP-2 (Table 4) shows that EURMAP-2 calculated results for $SO_4^=$ correlate with measurements somewhat better than the NILU calculated results; however, for SO_2, NILU results give higher correlation with measurements.

Table 8 shows r and r.m.s.e. values for NILU results for the September episode. A comparison of these values with those of EURMAP-2 results

Table 8. *Comparison between NILU-calculated and measured concentrations for SO_2 and $SO_4^=$ for September 1974 episode*

	September 14		September 15		September 16	
Pollutant	r	r.m.s.e. ($\mu g/m^3$)	r	r.m.s.e. ($\mu g/m^3$)	r	r.m.s.e. ($\mu g/m^3$)
SO_2	0.72	6.5	0.75	8.2	0.64	8.8
$SO_4^=$	0.76	3.0	0.74	3.7	0.79	5.6

(Table 6) shows that the NILU model correlates with measurements more consistently than the EURMAP-2 model, though for September 15 EURMAP-2 shows a higher correlation than NILU.

This study has not examined in detail the reasons for the differences in the performance of the EURMAP-2 and NILU models. However, we believe that these are perhaps a result of some significant differences in the treatment of certain important elements in the two models. Table 2 shows these differences for the long-term EURMAP-1, short-term EURMAP-2, and NILU models. Whereas NILU model characteristics are like those of the long-term EURMAP-1 model, they are significantly different from those of the short-term EURMAP-2 model; for example, the treatment of mixing height, transport wind, and vertical diffusion differs in the three models. The treatment of these and other elements in EURMAP-2 and EURMAP-1 is different because EURMAP-2 is specifically designed to simulate short-term (daily) episodic conditions. As such, it incorporates some physical characteristics that we believe to be necessary for simulating daily conditions but that can be simplified in long-term (monthly, seasonal, and annual) models such as EURMAP-1.

7. Conclusions

The regional air pollution model EURMAP-2 is designed for calculating short-term (daily) patterns of airborne sulfur over central and western Europe. This paper has presented a comparison between calculated and measured daily concentrations of SO_2 and $SO_4^=$. The comparison shows that the model-calculated concentrations are generally in reasonable agreement with the measurements over most of the model region. There are significant differences between calculated and measured concentrations in the eastern part of the region, which may be partly attributed to nonavailability of emissions from the eastern boundary of the model domain.

The EURMAP-2 model does not yet appear to show improvement over simpler models in regard to comparisons with the measurements. It does, however, contain more realistic features and is potentially more suitable for use in short-term episode calculations. The model in its present form does not incorporate the effect of complex terrain on transport and dry deposition processes. Other limitations of the model that can influence its performance pertain to the treatment of:

(a) Transformation rate
(b) Wet and dry deposition rates
(c) Rainfall over the North Sea
(d) Convergence and divergence in the wind-field.

The continued development of the EURMAP-2 model is now directed to obviate these limitations.

8. Acknowledgements

The research work described in this paper has been supported by the Federal Environmental Agency (Umweltbundesamt), Federal Republic of Germany. The authors are grateful for the assistance of Russell Trudeau of SRI International in the preparation of this paper.

REFERENCES

Bolin, B. and Persson, C. 1975. Regional dispersion and deposition of atmospheric pollutants with particular application to sulfur pollution over Western Europe. *Tellus 3*, 281–310.

Eliassen, A. and Saltbones, J. 1974. Decay and transformation rates of SO_2 as estimated from emission data, trajectories and measured air concentrations. *Atmos. Environ. 9*, 425–429.

Eliassen, A., Jensen, O. and Saltbones, J. 1976. *Model comparison using selected test-results with NILU (trajectory) model.* Report EMP 3/76 (November) Norwegian Institute for Air Research, Lillestrom, Norway.

Endlich, R. M. and Mancuso, R. L. 1968. Objective analysis of environmental conditions associated with severe thunderstorms and tornadoes. *Mon. Wea. Rev. 96*, 342–350.

Fisher, B. E. A. 1975. The long range transport of sulfur dioxide. *Atmos. Environ. 9*, 1063–1070.

Goodman, J. K. and Miller, A. 1977. Mass transport across a temperature inversion. *J. Geophys. Res. 82*, 3463–3471.

Holzworth, G. C. 1972. *Mixing heights, wind speeds, and potential for urban air pollution throughout the contiguous United States.* Environmental Protection Agency Report AP101, Washington, D.C., 118 pp. (Available from Superintendent of Documents, U.S. Government Printing Office, Washington, D.C.)

Johnson, W. B., Wolf, D. E. and Mancuso, R. L. 1978. Long term regional patterns and transfrontier exchanges of airborne sulfur pollution in Europe. *Atmos. Environ. 12*, 511-527.

Keyser, D. and Anthes, R. A. 1977. The applicability of a mixed layer model for the planetary boundary layer to real data forecasting. *Mon. Wea. Rev. 105*, 1351–1371.

Mancuso, R. L., Bhumralkar, C. M., Wolf, D. E. and Johnson, W. B. 1978. Evaluation and sensitivity analysis of the European Regional Model of Air Pollution (EURMAP-1). Progress Report, SRI Project 4797, Contract LUP 411 515/III A 315, SRI International, Menlo Park, California.

Maul, P. R. 1977. The mathematical model of the mesoscale transport of gaseous pollutants. *Atmos. Environ. 11*, 1191–1195.

NIAR 1975. *Final report of LRTAP data July–December 1974.* LRTAP 20/75, Norwegian Institute for Air Research, Kjeller, Norway.

OECD 1977. *The OECD program on long-range transport of air pollutants: Measurements and findings.* Organization for Economic Cooperation and Development (OECD), Paris, France.

Ottar, B. 1978. The OECD study on long range transport of air pollutants (LRTP). *Atmos. Environ. 12*, 445–454.

Prahm, L. P. and Christensen, O. 1977. Long range transmission of pollutants simulated by the 2-D pseudospectral dispersion model. *J. Appl. Meteor. 16*, 896–910.

Rao, K. S., Thomson, T. and Egan, B. A. 1976. Regional transport model of atmospheric sulfates. Proc. Annual Meeting of APCA, June 1976. Portland, Oregon, Paper No. 76-23·5.

Rystad, B., Stromsoe, S., Amble, E. and Knudsen, T. 1974. *The LRTAP emission survey.* LRTAP, Norwegian Institute for Air Research, Norway.

Sheih, C. M. 1977. Application of a statistical trajectory model to the simulation of sulfur pollution over the northeastern United States. *Atmos. Environ. 11*, 173–178.

Touma, J. S. 1977. Dependence of the wind profile power law on stability for various locations. *J. Air Poll. Contr. Assoc. 27*, 863–866.

Turner, D. B. 1970. *Workbook of atmospheric diffusion estimates.* Publication No. AP-26 Office of Air Programs, U.S. Environmental Protection Agency. Research Triangle Park, North Carolina, 89 pp.

РЕГИОНАЛЬНАЯ МОДЕЛЬ ЗАГРЯЗНЕНИЯ АТМОСФЕРЫ ДЛЯ ВЫЧИСЛЕНИЯ КОРОТКОПЕРИОДНЫХ (СУТОЧНЫХ) КАРТИН ЕГО РАСПРЕДЕЛЕНИЙ И ТРАНСГРАНИЧНЫХ ПЕРЕНОСОВ СЕРЫ В ЕВРОПЕ

Для моделирования и изучения эффектов суточных вариаций эмиссий серы на короткопериодные (суточные) изменения качества воздуха в центральной и западной Европе была разработана модель загрязнения атмосферы – EURMAP-2. Модель использовалась для расчета суточных концентраций, суточных отложений и суточных трансграничных переносов SO_2 и $SO_4^=$ в течение событий 25–26 августа и 14–16 сентября 1974 года. Сравнение между рассчитанными по модели и измеренными концентрациями SO_2 и $SO_4^=$ указывает на их довольно хорошее согласие в больших частях модельной сетки, хотя вычисленные концентрации ниже измеренных в ее восточных частях. Рассчитанные распределения сухих осаждений SO_2 выявляют сильную корреляцию с эмиссиями; распределения для влажных отложений близко соответствуют естественным неоднородностям в поле осадков. Различия между результатами по модели и по измерениям связываются с нерепрезентативностью данных по эмиссиям в восточной части области моделиро-

вания и с неспособностью модели реалистически описывать влияние сложной формы подстилающей поверхности, вертикальной диффузии, трансформации газов и скорости осаждения.

Сравнение между результатами EURMAP-2 и NILU (траекторной) модели, разработанной Норвежским институтом исследований воздуха, указывает на существенные различия, что, вероятно, есть результат различных трактовок некоторых физических процессов в этих моделях.